Study and validation of a variational theory of thermomechanical coupling in finite visco-plasticity

Laurent Stainier, Michael Ortiz

Study and validation of a variational theory of thermo-mechanical coupling in finite visco-plasticity

L. Stainier [a,*,1], M. Ortiz [b]

[a] Département Aérospatiale et Mécanique, Université de Liège, LTAS-MCT, Chemin des chevreuils 1, B-4000 Liège, Belgium
[b] Division of Engineering and Applied Science, California Institute of Technology, 1200 E. California Boulevard, MS 105-50, Pasadena, CA 91125, USA

We present an experimental validation of the variational theory of thermo-mechanical coupling of Yang et al. (2006) in the case of finite thermo-visco-plasticity. The variational theory results in precise *predictions* of the rate of heating due to dissipation and does not require an *a priori* definition or model of a fraction of plastic work converted to heat. We show that the *predicted* heat-to-plastic work ratios are in good agreement with experimental observations for 2024-T3 aluminum, α-titanium and pure polycrystalline tantalum, including their evolution with strain and their dependence on strain-rate. We also critically compare the variational theory to other theories and models in the literature.

1. Introduction

Thermo-mechanical coupling can significantly influence the plasticity of metals. This influence can extend to the entire body or be localized, e.g., within adiabatic shear bands. When the time of deformation is short, the thermo-mechanical process of plastic deformation can be reasonably approximated as adiabatic. However, under more general loading conditions thermal conductivity must be taken into consideration. Recently, a variational formulation of coupled thermo-mechanical problems has been proposed (Yang et al., 2006) that applies to a wide range of dissipative materials, including so-called generalized standard materials (Halphen and Nguyen, 1975). A testable difference between the variational and other theories of incremental finite thermo-visco-plasticity is the manner in which the intrinsic dissipation is computed. Thus, a standard practice in the case of finite thermo-visco-plasticity is to compute the intrinsic dissipation as a fraction of the power of plastic work (e.g., cf. Simo and Miehe, 1992; Marusich and Ortiz, 1995; Camacho and Ortiz, 1997; Nemat-Nasser et al., 1998; Adam and Ponthot, 2005; Rusinek et al., 2007). By way of sharp contrast, in the variational theory the intrinsic dissipation follows directly (and rigorously) from the free energy and dissipation potential, which also define hardening and rate-dependence behaviors, and need not – indeed cannot – be modeled independently. The *predicted* ratio of dissipation to plastic power is a function of strain level and strain-rate, in accordance with experiment (Taylor and Quinney, 1937; Titchener and Bever, 1958; Bever et al., 1973; Chrysochoos et al., 1989; Aravas et al., 1990; Zehnder, 1991; Chrysochoos and Belmahjoub, 1992; Mason et al., 1994; Zehnder et al., 1998; Hodowany et al., 2000; Benzerga et al., 2005; Jovic et al., 2006). Note that the value and evolution of the heat ratio of plastic power can have an influence on the development of shear instabilities in plastic materials (Charalambakis, 2001).

The principal objective of the present paper is to demonstrate the ability of the computational approach derived from the variational theory of coupled thermo-mechanical problems to provide accurate predictions of heating (resulting from the combined effect of dissipation and other entropic effects) in thermo-visco-plastic materials under various loading conditions. We base our validation on the experimental data of Hodowany et al. (2000) for 2024-T3 aluminum alloy and α-titanium, and of Rittel et al. (2007) for pure polycrystalline tantalum. Hodowany et al. conducted tests both in the quasi-static range and the dynamic range in a Kolsky bar configuration. The 2024-T3 aluminum alloy exhibited ostensibly rate-independent behavior whereas α-titanium exhibited strong rate-dependency effects. Rittel et al. (2007) also tested polycrystalline tantalum samples both in the quasi-static range and the highly dynamic range using a shear-compression configuration. These experimental studies supply a wealth of experimental data for purposes of validation of thermo-mechanical coupling theories. The good overall agreement reported in this paper between the observational data and the predictions of the variational approach lends strong support to the latter. We also discuss the relation between the variational theory and other theories proposed in the literatures (Chaboche, 1993; Rosakis et al., 2000; Longère and Dragon, 2008a,b; Rusinek and Klepaczko, 2009).

* Corresponding author.
E-mail address: Laurent.Stainier@ec-nantes.fr (L. Stainier).
[1] Present address: GeM (UMR CNRS 6183), Ecole Centrale de Nantes, 1 rue de la Noë, BP 92101, F-44321 Nantes, France.

2. The variational model of finite thermo-visco-plasticity

We begin by summarizing the variational formulation of the finite thermo-visco-plasticity constitutive equations. The formulation of the corresponding dynamical boundary value problem and time discretizations thereof, including the formulation variational thermo-visco-plastic constitutive updates, may be found in Yang et al. (2006).

2.1. Thermodynamic framework

Viscoplastic solids are characterized by the existence of a certain class of deformations $\boldsymbol{F}^{\mathrm{p}}$, or *plastic* deformations, which leave the crystal lattice undistorted and unrotated, and, consequently, induce no long-range stresses. In addition to the plastic deformation $\boldsymbol{F}^{\mathrm{p}}$, some degree of lattice distortion $\boldsymbol{F}^{\mathrm{e}}$, or *elastic* deformation, may also be expected in general. One therefore has, locally,

$$\boldsymbol{F} = \boldsymbol{F}^{\mathrm{e}}\boldsymbol{F}^{\mathrm{p}} \tag{1}$$

This multiplicative elastic–plastic kinematics was first suggested by Lee (1969), and further developed and used by many others. In this paper, we consider macroscopic models of plasticity of the von Mises type. These can be characterized by a plastic flow rule of the form

$$\boldsymbol{L}^{\mathrm{p}} = \dot{\boldsymbol{F}}^{\mathrm{p}}\boldsymbol{F}^{\mathrm{p}-1} = \boldsymbol{D}^{\mathrm{p}} = \dot{\bar{\epsilon}}^{\mathrm{p}}\boldsymbol{M} \quad \text{with } \mathrm{tr}[\boldsymbol{M}] = 0 \text{ and } \boldsymbol{M}\cdot\boldsymbol{M} = \frac{3}{2} \tag{2}$$

where $\bar{\epsilon}^{\mathrm{p}}$ is a scalar internal variable measuring the cumulated plastic strain, and $\boldsymbol{M}$ is a traceless normalized symmetric tensor. The constraints on $\boldsymbol{M}$ embody the incompressibility of plastic flow and the hypothesis of zero plastic spin. The tensor $\boldsymbol{M}$ is not defined further at this point and follows from the variational principle detailed below. Thus, in the present framework the set of internal variables is $\boldsymbol{Z} = \{\boldsymbol{F}^{\mathrm{p}}, \bar{\epsilon}^{\mathrm{p}}\}$, which is subject to the non-holonomic constraint (2).

Note that in the variational approach no yield function or surface is explicitly introduced, contrary to more traditional approaches. Instead we assume a particular kinematics of the plastic flow, as expressed by the choice of the flow rule (2). As it will become apparent later, the choice of a traceless, symmetric, plastic velocity gradient $\boldsymbol{L}^{\mathrm{p}}$ leads to a model of the von Mises type. In particular, the setting of the plastic spin to zero is a simple choice at the level of kinematics. Other choices are possible, corresponding for example to Tresca type or crystal plasticity, as illustrated in Ortiz and Stainier (1999).

We postulate the existence of a Helmholtz free energy density of the form

$$W = W(\boldsymbol{F}^{\mathrm{e}}, \boldsymbol{F}^{\mathrm{p}}, \bar{\epsilon}^{\mathrm{p}}, T) = W\left(\boldsymbol{F}\boldsymbol{F}^{\mathrm{p}-1}, \boldsymbol{F}^{\mathrm{p}}, \bar{\epsilon}^{\mathrm{p}}, T\right) \equiv W(\boldsymbol{F}, \boldsymbol{F}^{\mathrm{p}}, \bar{\epsilon}^{\mathrm{p}}, T) \tag{3}$$

We shall denote by $\boldsymbol{P}$ the first Piola–Kirchhoff stress tensor. It follows from Coleman's relations as:

$$\boldsymbol{P} = \frac{\partial W}{\partial \boldsymbol{F}}(\boldsymbol{F}, \boldsymbol{F}^{\mathrm{p}}, \bar{\epsilon}^{\mathrm{p}}, T) \tag{4}$$

The tacit assumption in writing (3) is that

$$W_{,\boldsymbol{F}}(\boldsymbol{F}^{\mathrm{e}} = \boldsymbol{I}, \boldsymbol{F}^{\mathrm{p}}, \bar{\epsilon}^{\mathrm{p}}, T) = \boldsymbol{0} \tag{5}$$

i.e., that the solid fully relaxes its free energy when its plastic deformation $\boldsymbol{F}^{\mathrm{p}}$ exactly matches the overall imposed deformation $\boldsymbol{F}$. However, the kinematics of plastic flow, as embodied in the plastic flow rule defined above, generally results in incompatible plastic deformation fields. This incompatibility prevents the full plastic relaxation of the free energy and the material becomes stressed. The entropy density per unit undeformed volume is given by:

$$\rho_0\eta = -\frac{\partial W}{\partial T}(\boldsymbol{F}, \boldsymbol{F}^{\mathrm{p}}, \bar{\epsilon}^{\mathrm{p}}, T) \tag{6}$$

where η is the specific entropy, and ρ_0 the mass density in the undeformed configuration. The heat capacity at constant strain and constant internal state is defined as

$$\rho_0 C = -T\frac{\partial^2 W}{\partial T^2}(\boldsymbol{F}, \boldsymbol{F}^{\mathrm{p}}, \bar{\epsilon}^{\mathrm{p}}, T) \tag{7}$$

where C is the specific heat capacity. It corresponds to the specific heat capacity at constant volume as classically defined for thermodynamics of gases. The specific internal energy per unit undeformed volume can be defined from the free energy by means of the Legendre–Fenchel transform:

$$U(\boldsymbol{F}, \boldsymbol{F}^{\mathrm{p}}, \bar{\epsilon}^{\mathrm{p}}, \eta) = \sup_{T}\left[\rho_0\eta T + W(\boldsymbol{F}, \boldsymbol{F}^{\mathrm{p}}, \bar{\epsilon}^{\mathrm{p}}, T)\right] \tag{8}$$

The internal energy function is a state function, i.e., in the sense that it depends on the current material state only.

In materials such as metals, the elastic response and the specific heat are ostensibly independent of the internal processes and the free energy (3) decomposes additively as

$$W = W^{\mathrm{e}}\left(\boldsymbol{F}\boldsymbol{F}^{\mathrm{p}-1}, T\right) + W^{\mathrm{p}}(\boldsymbol{F}^{\mathrm{p}}, \bar{\epsilon}^{\mathrm{p}}, T) + W^{\mathrm{h}}(T) \tag{9}$$

The function W^{e} determines the elastic response of the metal, e.g., upon unloading, whereas the function W^{p} represents the stored energy due to the plastic working of the material. The thermal energy W^{h} describes the heat storage capacity of the material. Considerations on frame indifference (objectivity) impose a specific form to the dependence of the elastic energy on the elastic strain tensor:

$$W^{\mathrm{e}}(\boldsymbol{F}^{\mathrm{e}}, T) \equiv W^{\mathrm{e}}(\boldsymbol{C}^{\mathrm{e}}, T) \quad \text{with} \quad \boldsymbol{C}^{\mathrm{e}} = \boldsymbol{F}^{\mathrm{e}T}\boldsymbol{F}^{\mathrm{e}} \tag{10}$$

where $\boldsymbol{C}^{\mathrm{e}}$ is the elastic right Cauchy–Green strain tensor. The case in which W^{p} depends explicitly on $\boldsymbol{F}^{\mathrm{p}}$ is known as kinematic hardening. The back-stress tensor:

$$\boldsymbol{T}^{c} = \frac{\partial W^{\mathrm{p}}}{\partial \boldsymbol{F}^{\mathrm{p}}}(\boldsymbol{F}^{\mathrm{p}}, \bar{\epsilon}^{\mathrm{p}}, T) \tag{11}$$

represents a shift in the plastic flow potential, or the elastic domain in the rate-independent limit, as we will see later. The force thermodynamically conjugate to the plastic strain $\boldsymbol{F}^{\mathrm{p}}$ is then given by:

$$\boldsymbol{T} = -\frac{\partial W}{\partial \boldsymbol{F}^{\mathrm{p}}} = \boldsymbol{F}^{\mathrm{e}T}\boldsymbol{P} - \boldsymbol{T}^{c} \tag{12}$$

Accounting for the flow rule (2), the force thermodynamically conjugate to the cumulated plastic strain is

$$Y = -\frac{\partial W}{\partial \bar{\epsilon}^{\mathrm{p}}} = \boldsymbol{T}\cdot(\boldsymbol{M}\boldsymbol{F}^{\mathrm{p}}) - \frac{\partial W^{\mathrm{p}}}{\partial \bar{\epsilon}^{\mathrm{p}}} \tag{13}$$

Note that in deriving Y use has been made of the non-holonomic constraint (2) expressing the flow rule.

In order to determine the evolution of the internal variable $\bar{\epsilon}^{\mathrm{p}}$, a suitable kinetic equation must be provided. Assuming that the rate of the local internal processes described by $\bar{\epsilon}^{\mathrm{p}}$ is determined solely by the local thermodynamic state, the general form of the kinetic equation is

$$\dot{\bar{\epsilon}}^{\mathrm{p}} = f(\boldsymbol{F}, \boldsymbol{F}^{\mathrm{p}}, \bar{\epsilon}^{\mathrm{p}}, T) \tag{14}$$

A traditional approach is to consider that this kinetic relation can be derived from a dissipation pseudo-potential $\psi(Y)$:

$$\dot{\bar{\epsilon}}^{\mathrm{p}} = \frac{\partial \psi}{\partial Y}(Y; \boldsymbol{F}, \boldsymbol{F}^{\mathrm{p}}, \bar{\epsilon}^{\mathrm{p}}, T) \tag{15}$$

where the list of arguments after the semi-column indicates a possible parametric dependence on the current local thermodynamic state. Then, convexity of the pseudo-potential ψ in Y ensures the positivity of the intrinsic dissipation $\mathscr{D}^{\mathrm{int}} = Y\dot{\bar{\epsilon}}^{\mathrm{p}}$. Dual dissipation

pseudo-potential can be defined by recourse to a Legendre–Fenchel transform:

$$\psi^*\left(\dot{\bar{\epsilon}}^{\mathrm{p}};\boldsymbol{F},\boldsymbol{F}^{\mathrm{p}},\bar{\epsilon}^{\mathrm{p}},T\right)=\sup_{Y}\left[Y\dot{\bar{\epsilon}}^{\mathrm{p}}-\psi(Y;\boldsymbol{F},\boldsymbol{F}^{\mathrm{p}},\bar{\epsilon}^{\mathrm{p}},T)\right] \tag{16}$$

Convexity of $\psi(Y)$ implies convexity of $\psi^*(\dot{\bar{\epsilon}}^{\mathrm{p}})$, and the kinetic relation can take the alternate form:

$$Y=\frac{\partial\psi^*}{\partial\dot{\bar{\epsilon}}^{\mathrm{p}}}\left(\dot{\bar{\epsilon}}^{\mathrm{p}};\boldsymbol{F},\boldsymbol{F}^{\mathrm{p}},\bar{\epsilon}^{\mathrm{p}},T\right) \tag{17}$$

Finally, the conservation law for energy can be written in entropy form:

$$\rho_0\dot{\eta}=\frac{1}{T}\left[Y\dot{\bar{\epsilon}}^{\mathrm{p}}-\mathrm{Div}\boldsymbol{H}+\rho_0 Q\right] \tag{18}$$

where $\boldsymbol{H}$ is the heat flux vector and Q denotes an external volumic heat source. In the sequel we will restrict ourselves to the *adiabatic* case, i.e., the case in which there are no external heat sources ($Q=0$) and the heat flux is negligible. Conservation of energy then yields

$$\rho_0\dot{\eta}=\frac{1}{T}Y\dot{\bar{\epsilon}}^{\mathrm{p}}=\frac{1}{T}\mathscr{D}^{\mathrm{int}} \tag{19}$$

It should be carefully noted that heat conduction can be readily included in the variational formulation (see Yang et al., 2006). However, heat conduction does not essentially alter the discussion that follows and hence will be removed from consideration in the interest of simplicity.

2.2. Variational formulation

The above constitutive equations can be restated in a variational framework, as explained in Ortiz and Stainier (1999) and Yang et al. (2006). To this end, we introduce the power density function

$$\mathscr{D}\left(\dot{\boldsymbol{F}},\dot{\bar{\epsilon}}^{\mathrm{p}},\boldsymbol{M},\dot{\eta},T;\boldsymbol{F},\boldsymbol{F}^{\mathrm{p}},\bar{\epsilon}^{\mathrm{p}},\eta\right)=\dot{U}-\rho_0\dot{\eta}T+\psi^*\left(\frac{T}{\Theta}\dot{\bar{\epsilon}}^{\mathrm{p}};\boldsymbol{F},\boldsymbol{F}^{\mathrm{p}},\bar{\epsilon}^{\mathrm{p}},\Theta\right) \tag{20}$$

where $\Theta(\boldsymbol{F},\boldsymbol{F}^{\mathrm{p}},\bar{\epsilon}^{\mathrm{p}},\eta)=\partial U/\partial(\rho_0\eta)$ is regarded as an equation of state derived from the internal energy. Then, constitutive relations (17) and (19) can be restated under the variational form:

$$\mathscr{D}^{\mathrm{eff}}\left(\dot{\boldsymbol{F}},T;\boldsymbol{F},\boldsymbol{F}^{\mathrm{p}},\bar{\epsilon}^{\mathrm{p}},\eta\right)=\inf_{\dot{\bar{\epsilon}}^{\mathrm{p}},\boldsymbol{M},\dot{\eta}}\mathscr{D}\left(\dot{\boldsymbol{F}},\dot{\bar{\epsilon}}^{\mathrm{p}},\boldsymbol{M},\dot{\eta},T;\boldsymbol{F},\boldsymbol{F}^{\mathrm{p}},\bar{\epsilon}^{\mathrm{p}},\eta\right) \tag{21}$$

The optimality condition with respect to $\dot{\eta}$ yields

$$T=\frac{\partial U}{\partial(\rho_0\eta)}=\Theta(\boldsymbol{F},\boldsymbol{F}^{\mathrm{p}},\bar{\epsilon}^{\mathrm{p}},\eta) \tag{22}$$

stating that the "external" temperature T is equal to the "internal" temperature Θ.[2] Then, the optimality condition on $\dot{\bar{\epsilon}}^{\mathrm{p}}$ yields

$$\frac{\partial U}{\partial\bar{\epsilon}^{\mathrm{p}}}(\boldsymbol{F},\boldsymbol{F}^{\mathrm{p}},\bar{\epsilon}^{\mathrm{p}},\eta)+\frac{\partial\psi^*}{\partial\dot{\bar{\epsilon}}^{\mathrm{p}}}\left(\dot{\bar{\epsilon}}^{\mathrm{p}};\boldsymbol{F},\boldsymbol{F}^{\mathrm{p}},\bar{\epsilon}^{\mathrm{p}},\Theta\right)=0 \tag{23}$$

which is equivalent to the kinetic equation (17). Finally, the plastic flow direction $\boldsymbol{M}$ is given by

$$\max_{\boldsymbol{M}}\left(\boldsymbol{T}\boldsymbol{F}^{\mathrm{p}T}\right)\cdot\boldsymbol{M}\dot{\bar{\epsilon}}^{\mathrm{p}}\quad\text{subject to }\boldsymbol{M}\cdot\boldsymbol{M}=\frac{3}{2}\ \text{ and }\ \mathrm{tr}[\boldsymbol{M}]=0 \tag{24}$$

which yields

$$\boldsymbol{M}=\sqrt{\frac{3}{2}}\frac{\mathrm{dev}[\boldsymbol{S}-\boldsymbol{S}^c]}{\|\mathrm{dev}[\boldsymbol{S}-\boldsymbol{S}^c]\|} \tag{25}$$

[2] Note that, from a theoretical point of view, one could also consider the introduction of a dissipation pseudo-potential function of $\dot{\eta}$, corresponding to a non-equilibrium approach to the thermal problem. But the physical significance of such a potential remains to be explored.

where $\boldsymbol{S}=\boldsymbol{F}^{\mathrm{e}T}\boldsymbol{P}\boldsymbol{F}^{\mathrm{p}T}$ is the Mandel stress tensor and $\boldsymbol{S}^c=\boldsymbol{T}^c\boldsymbol{F}^{\mathrm{p}T}$. Introducing the above result in (13) gives

$$Y=\sqrt{\frac{3}{2}}\|\boldsymbol{S}-\boldsymbol{S}^c\|-\frac{\partial W^{\mathrm{p}}}{\partial\bar{\epsilon}^{\mathrm{p}}} \tag{26}$$

which relates Y to the equivalent stress computed from Mandel stress tensor.

Note that, in writing (25), we implicitly assume the symmetry of $\boldsymbol{S}$ and $\boldsymbol{S}^c$. In the general case, the expression of $\boldsymbol{M}$ should be more rigorously written as proportional to the deviator of the symmetric part of $\boldsymbol{S}-\boldsymbol{S}^c$. In the examples below, though, we only consider isotropic materials for which the symmetry of Mandel stress tensor is automatically verified.

Taking into account the above optimality conditions, it is easily verified that the resulting function $\mathscr{D}^{\mathrm{eff}}$ plays the role of a rate potential:

$$\frac{\partial\mathscr{D}^{\mathrm{eff}}}{\partial\dot{\boldsymbol{F}}}=\frac{\partial U}{\partial\boldsymbol{F}}(\boldsymbol{F},\boldsymbol{F}^{\mathrm{p}},\bar{\epsilon}^{\mathrm{p}},\eta)=\boldsymbol{P} \tag{27}$$

$$\frac{\partial\mathscr{D}^{\mathrm{eff}}}{\partial T}=-\rho_0\dot{\eta}+\frac{1}{\Theta}\frac{\partial\psi^*}{\partial\dot{\bar{\epsilon}}^{\mathrm{p}}}\left(\dot{\bar{\epsilon}}^{\mathrm{p}};\boldsymbol{F},\boldsymbol{F}^{\mathrm{p}},\bar{\epsilon}^{\mathrm{p}},\Theta\right)\dot{\bar{\epsilon}}^{\mathrm{p}}=-\rho_0\dot{\eta}+\frac{1}{\Theta}Y\dot{\bar{\epsilon}}^{\mathrm{p}} \tag{28}$$

Comparing (19) and (28), it follows that the adiabatic energy conservation equation can be rewritten as

$$\partial\mathscr{D}^{\mathrm{eff}}/\partial T=0 \tag{29}$$

in terms of the rate potential $\mathscr{D}^{\mathrm{eff}}$. Thus, $\mathscr{D}^{\mathrm{eff}}$ defines a joint potential for the effective stress-deformation relations and the energy balance equation.

2.3. Plastic work partition

As mentioned earlier, the heat capacity (at constant deformation and internal variables) is defined as

$$\rho_0 C=-T\frac{\partial^2 W}{\partial T^2}(\boldsymbol{F},\boldsymbol{F}^{\mathrm{p}},\bar{\epsilon}^{\mathrm{p}},T) \tag{30}$$

Note that the heat capacity C is not constant in general. The adiabatic heat equation (19), can then be rewritten as

$$\rho_0 C\dot{T}=T\frac{\partial\boldsymbol{P}}{\partial T}\cdot\dot{\boldsymbol{F}}-T\frac{\partial Y}{\partial T}\dot{\bar{\epsilon}}^{\mathrm{p}}+Y\dot{\bar{\epsilon}}^{\mathrm{p}} \tag{31}$$

The first term on the right-hand side represents the contribution to heating from thermoelastic effects, as well as softening of elastic moduli. The second term represents contributions from plastic softening, while the third term is the contribution of the intrinsic dissipation $\mathscr{D}^{\mathrm{int}}$. For metals undergoing large plastic strains, the first two contributions are typically small when compared to the third one, and are thus often neglected in the literature. In the variational formulation though, heat equation is solved under its entropic form (19) (or its incremental equivalent), and all contributions are thus naturally taken into account. In the case of finite plastic strains, the main contribution to the adiabatic heat equation (31) thus comes from the intrinsic dissipation $\mathscr{D}^{\mathrm{int}}=Y\dot{\bar{\epsilon}}^{\mathrm{p}}$. Using (12) and (13), one can write

$$\mathscr{D}^{\mathrm{int}}\equiv Y\dot{\bar{\epsilon}}^{\mathrm{p}}=\left[(\boldsymbol{S}-\boldsymbol{S}^c)\cdot\boldsymbol{M}-\frac{\partial W^{\mathrm{p}}}{\partial\bar{\epsilon}^{\mathrm{p}}}\right]\dot{\bar{\epsilon}}^{\mathrm{p}}=(\boldsymbol{S}-\boldsymbol{S}^c)\cdot\boldsymbol{D}^{\mathrm{p}}-\frac{\partial W^{\mathrm{p}}}{\partial\bar{\epsilon}^{\mathrm{p}}}\dot{\bar{\epsilon}}^{\mathrm{p}} \tag{32}$$

Relation (32) can be formally rewritten in the form:

$$\mathscr{D}^{\mathrm{int}}=\beta\boldsymbol{S}\cdot\boldsymbol{D}^{\mathrm{p}} \tag{33}$$

where β represents the ratio of the intrinsic rate of dissipation to the total plastic power. In their pioneering work, Taylor and Quinney (1937) conducted an experimental study of heating due to plastic

work, and found that the fraction β was typically in the range [0.8, 1.0] for the materials they studied (see also Titchener and Bever, 1958; Bever et al., 1973). On the basis of these experimental results, many authors in subsequent works (e.g., Simo and Miehe, 1992; Marusich and Ortiz, 1995; Camacho and Ortiz, 1997; Nemat-Nasser et al., 1998; Adam and Ponthot, 2005; Rusinek et al., 2007) have approximated the intrinsic dissipation by expression (33) with a constant coefficient β. The assumption of a constant β is a rather crude one in general, as demonstrated by more recent experimental work (Chrysochoos et al., 1989; Chrysochoos and Belmahjoub, 1992; Mason et al., 1994; Zehnder et al., 1998; Hodowany et al., 2000; Jovic et al., 2006). Indeed, these experimental studies, using various techniques, concur in showing significant variations of the heat to plastic work ratio with both strain and strain-rate. A number of authors have derived models for the evolution of the factor β with strain and strain-rate, with a macroscopic point of view (Chaboche, 1993; Rosakis et al., 2000; Longère and Dragon, 2008a,b; Rusinek and Klepaczko, 2009), or even starting from microscopic considerations (Aravas et al., 1990; Zehnder, 1991; Benzerga et al., 2005). In the thermodynamical modelling framework adopted here, however, relation (32) shows that that evolution is entirely determined by the choice of potentials W^{p} and ψ^*. The variational formulation presented above is directly based on these potentials and thus sidesteps the need to partition plastic work and supply an explicit model of the factor β in order to compute the local temperature change. It should be carefully noted, however, that such partition can nonetheless be computed *a posteriori* if desired.

It should be carefully noted that expression (32) for the intrinsic dissipation is derived here merely as a basis for the discussion of the so-called Taylor–Quinney factor, and is not germane to the variational theory. In practice, the variational approach calculates the adiabatic heating directly from (29), or an incremental time-discretized version thereof, consistently with the full adiabatic heat equation (31). It should be carefully noted as well that (27) and (28) actually account for all sources of thermo-mechanical coupling and are not restricted to adiabatic heating.

2.4. Numerical aspects

Details of the time-discrete variational formulation and its numerical implementation fall outside the scope of this paper, and have been discussed elsewhere (Yang et al., 2006; Kulkarni et al., 2008; Stainier, 2009). Let us simply indicate that, in the discrete setting, the variational approach leads to a fully implicit and symmetric formulation, ensuring unconditional stability and excellent convergence properties (see for example Stainier, 2007). More generally, the variational structure confers the resulting algorithms very good robustness properties, which have been verified *de facto* in test cases involving thermoplasticity (e.g., Stainier, 2009).

3. Comparison with experimental results

Experimental observations suggest that the heat capacity of metals is not influenced by work hardening, which, by consideration of (7), imposes a dependence of W^{p} on T which is at most linear. Similarly, both experimental observations and theoretical analysis (Weiner, 2002) indicate a linear dependence of elastic constants with respect to the temperature. In accordance with these remarks, we will consider the following free energies:

$$W^{\mathrm{e}}(\boldsymbol{C}^{\mathrm{e}},T)=\frac{1}{2}K(T)(\mathrm{tr}[\boldsymbol{\epsilon}^{\mathrm{e}}])^2+G(T)(\mathrm{dev}[\boldsymbol{\epsilon}^{\mathrm{e}}]\cdot\mathrm{dev}[\boldsymbol{\epsilon}^{\mathrm{e}}])-3K_0\alpha(T-T_0)\log J \tag{34}$$

$$W^{\mathrm{p}}(\bar{\epsilon}^{\mathrm{p}},T)=\frac{n}{n+1}\frac{\sigma_0(T)}{b}(1+b\bar{\epsilon}^{\mathrm{p}})^{\frac{1}{n}+1}+\hat{\sigma}_0(T)\left[\bar{\epsilon}^{\mathrm{p}}+\frac{1}{d}\exp\left(-d\bar{\epsilon}^{\mathrm{p}}\right)\right] \tag{35}$$

$$W^{\mathrm{h}}(T)=\rho_0 C_0 T\left(1-\log\frac{T}{T_0}\right) \tag{36}$$

where $\boldsymbol{\epsilon}^{\mathrm{e}}=\log\left[\sqrt{\boldsymbol{C}^{\mathrm{e}}}\right]$ and $J=\det\left[\sqrt{\boldsymbol{C}^{\mathrm{e}}}\right]=\det[\boldsymbol{F}]$. Elastic moduli are given by

$$K(T)=K_0-K_1(T-T_0) \tag{37}$$

$$G(T)=G_0-G_1(T-T_0) \tag{38}$$

where T_0 is the initial temperature. The third term in (34) accounts for thermoelastic coupling (thermal dilatation coefficient α). The plastic free energy W^{p} is composed of a power-law term and an exponential saturation term. In accordance with above remarks, critical stresses σ_0 and $\hat{\sigma}_0$ are given by

$$\sigma_0(T)=\sigma_0(T_0)[1-\omega_0(T-T_0)] \tag{39}$$

$$\hat{\sigma}_0(T)=\hat{\sigma}_0(T_0)[1-\hat{\omega}_0(T-T_0)] \tag{40}$$

The dissipation pseudo-potential ψ^* can also be given a general expression of the form:

$$\psi^*\left(\dot{\bar{\epsilon}}^{\mathrm{p}};\bar{\epsilon}^{\mathrm{p}},T\right)=\sigma_y(\bar{\epsilon}^{\mathrm{p}},T)\dot{\bar{\epsilon}}^{\mathrm{p}}+\frac{m}{m+1}\sigma_v(T)\dot{\epsilon}_0\left(\frac{\dot{\bar{\epsilon}}^{\mathrm{p}}}{\dot{\epsilon}_0}\right)^{\frac{1}{m}+1} \tag{41}$$

where

$$\sigma_y(\bar{\epsilon}^{\mathrm{p}},T)=\sigma_1(T)\left(1+b'\bar{\epsilon}^{\mathrm{p}}\right)^{\frac{1}{n'}}+\hat{\sigma}_1(T)\left[1-\exp\left(-d'\bar{\epsilon}^{\mathrm{p}}\right)\right] \tag{42}$$

The dissipation pseudo-potential (41) is composed of a rate-independent term (homogeneous of order 1 in $\dot{\bar{\epsilon}}^{\mathrm{p}}$) and a rate-dependent term (power-law). The former part is itself composed of a power-law term and an exponential saturation term. Critical stresses σ_1, $\hat{\sigma}_1$ and σ_v are given by

$$\sigma_1(T)=\sigma_1(T_0)[1-\omega_1(T-T_0)] \tag{43}$$

$$\hat{\sigma}_1(T)=\hat{\sigma}_1(T_0)[1-\hat{\omega}_1(T-T_0)] \tag{44}$$

$$\sigma_v(T)=\sigma_v(T_0)[1-\omega_v(T-T_0)] \tag{45}$$

Other parameters $(b',d',n',m,\dot{\epsilon}_0)$ could be chosen as dependent on temperature as well, but for the sake of simplicity, we will take them constant here (a temperature-dependent $\dot{\epsilon}_0(T)$ will be introduced in the specific case of tantalum, see below).

We now proceed to check if general expressions (34), (35) and (41) for the constitutive potentials allow to reproduce experimental observations by numerical simulation. In particular, we will consider experimental measures by Hodowany et al. (2000), who conducted tests both in the quasi-static range and the dynamic range (Kolsky bar). They studied a 2024-T3 aluminum alloy, which proved to exhibit a rate-independent behavior, and α-titanium, showing strong rate-dependency effects. We complete the study by considering recent experimental results by Rittel et al. (2007), obtained on pure polycrystalline tantalum samples, again both in the quasi-static range and the highly dynamic range (shear-compression specimen).

3.1. Aluminum

The rate-independency observed in the behavior of the aluminum alloy allows to reduce the number of parameters from the onset. Then, a rather simple identification procedure, consisting in fitting numerical stress–strain and temperature–strain curves to experimental ones (see Figs. 1 and 2), yields the set of constitutive parameters listed in Table 1. Note that the available experimental data did not allow to quantify the temperature-dependence of elastic moduli, which were thus taken as constants. Note also that the parameters related to the rate-dependent part of the dissipation pseudo-potential (41) are not relevant in this case, and that the dissipation term actually reduces to a simple linear hardening contribution (with thermal softening).

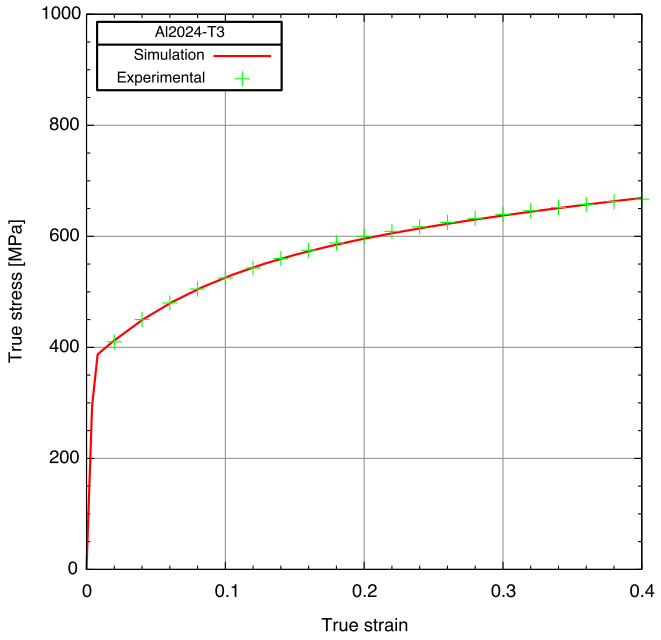

Fig. 1. Stress–strain curve for rate-independent 2023-T3 aluminum alloy. Experimental results taken from Hodowany et al. (2000).

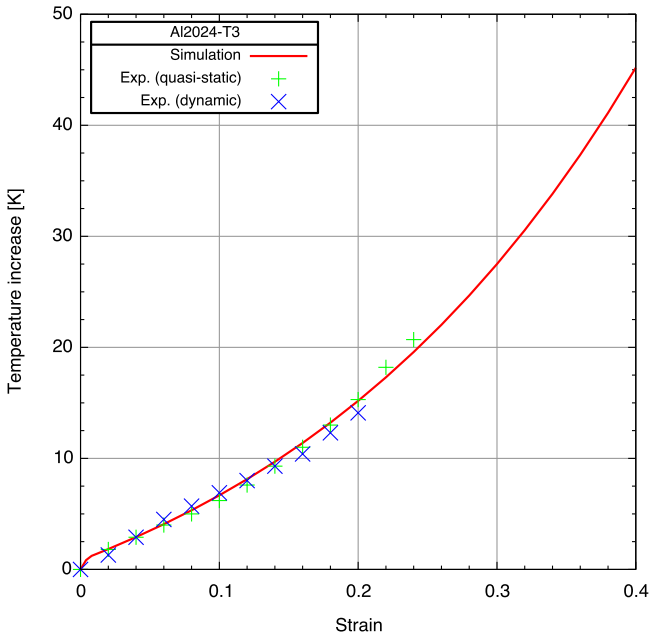

Fig. 2. Adiabatic heating curve for rate-independent 2023-T3 aluminum alloy. Experimental results taken from Hodowany et al. (2000).

3.2. Titanium

A similar identification procedure was carried out for the α-titanium alloy, using this time rate-dependent stress–strain and temperature–strain curves (see Figs. 3 and 4). The fitting is a little less precise than in the previous case, at least on the stress–strain curves, but we do not think that this significantly affects the discussion below. The resulting set of constitutive parameters is given in Table 2. Note that, in the high strain-rate case, experimental results are limited to a strain range of 20%, with a direct consequence on the precision of the identification in that case. These cautionary remarks should not prevent a qualitative analysis of the obtained results, though.

3.3. Tantalum

Tantalum exhibits significant strain-rate sensitivity, and its behavior is strongly temperature-dependent, as observed in numerous experimental studies. Among others, we can refer to the works of Hoge and Mukherjee (1977), Nemat-Nasser and Isaacs (1997) and Kapoor and Nemat-Nasser (1998), or more recently Rittel et al. (2007). All these authors studied polycrystalline tantalum samples, but of varying grades and purity levels. On the other hand, many constitutive models have been proposed to reproduce these experimental observations through numerical simulation (a non-exhaustive list would notably include Zerilli and Armstrong (1990), Chen and Gray (1996), Khan and Liang (1999, 2000), Nemat-Nasser and Kapoor (2001) and Voyiadjis and Abed (2005, 2006)).

In this work, since our goal is mainly to demonstrate the capacity of the proposed variational formulation to catch the salient features of thermo-plastic coupling, we will proceed with the general model described by (34), (35) and (41). To take into account the specificities of tantalum behavior, and inspired by our own previous work on tantalum single crystals (Stainier et al., 2002) (see also Lee et al., 1997 or Kothari and Anand, 1998), we will consider that the temperature-dependence of parameters describing the rate-dependent part of (41) is controlled by a thermally activated process (motion of dislocations through Peierls barriers):

$$\sigma_v(T) = \sigma_v(T_0)\frac{T}{T_0} \tag{46}$$

$$\dot{\epsilon}_0(T) = \dot{\epsilon}_0(T_0)\exp\left[-T_c\left(\frac{1}{T}-\frac{1}{T_0}\right)\right] \tag{47}$$

where $T_c = E_a/k_B$ is a characteristic temperature, defined from the activation energy E_a and Boltzmann constant k_B.

Table 1
Material properties for rate-independent 2024-T3 aluminum alloy ($T_0 = 293$ K).

G_0 (GPa)	G_1 (GPa/K)	K_0 (GPa)	K_1 (GPa/K)	α (K^{-1})	ρ_0 (kg/m^3)	C_0 (J/(kg K))
27.5	0.0	71.7	0.0	24.7×10^{-6}	2780.0	875.0
$\sigma_0(T_0)$ (MPa)	ω_0 (K^{-1})	b	n	$\hat{\sigma}_0(T_0)$ (MPa)	$\hat{\omega}_0$ (K^{-1})	d
255.0	0.0	−1.0	1.5	170.0	0.0	12.0
$\sigma_1(T_0)$ (MPa)	ω_1 (K^{-1})	b'	n'	$\hat{\sigma}_1(T_0)$ (MPa)	$\hat{\omega}_1$ (K^{-1})	d'
125.0	0.0007	4.0	1.0	0.0	–	–
$\sigma_v(T_0)$ (MPa)	ω_v (K^{-1})	$\dot{\epsilon}_0$ (s^{-1})	m			
0.0	–	–	–			

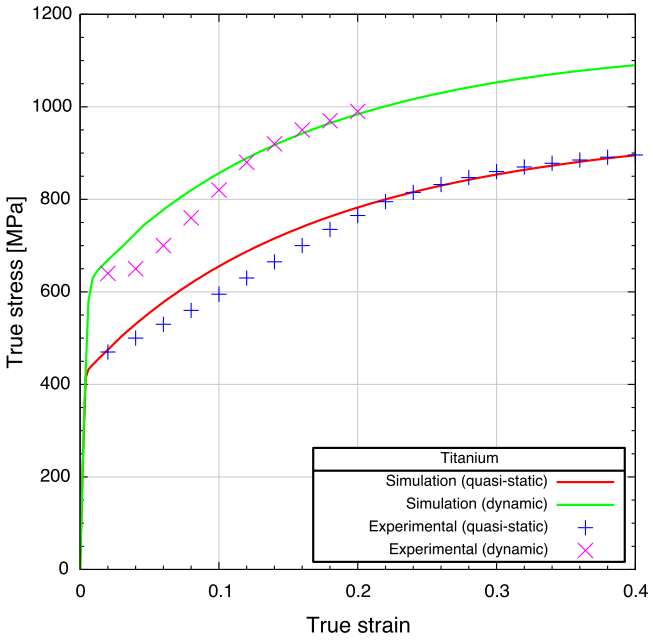

Fig. 3. Stress–strain curve at two different strain rates (quasi-static at 10^{-3} s^{-1} and dynamic at 3000 s^{-1}) for rate-dependent α-titanium alloy. Experimental results taken from Hodowany et al. (2000).

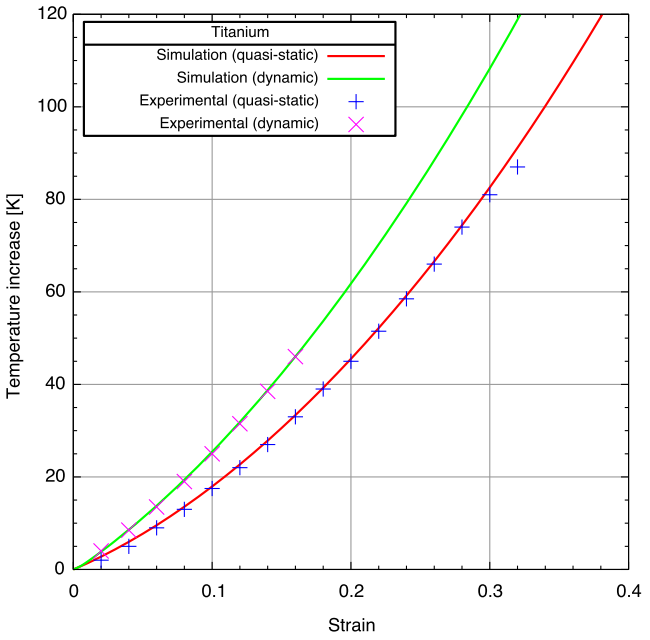

Fig. 4. Adiabatic heating curve at two different strain rates (quasi-static at 10^{-3} s^{-1} and dynamic at 3000 s^{-1}) for rate-dependent α-titanium alloy. Experimental results taken from Hodowany et al. (2000).

Table 2
Material properties for rate-dependent α-titanium alloy ($T_0 = 293$ K).

G_0 (GPa)	G_1 (GPa/K)	K_0 (GPa)	K_1 (GPa/K)	α (K^{-1})	ρ_0 (kg/m^3)	C_0 (J/(kg K))
43.0	0.0	128.9	0.0	8.9×10^{-6}	4500.0	518.0
$\sigma_0(T_0)$ (MPa)	ω_0 (K^{-1})	b	n	$\hat{\sigma}_0(T_0)$ (MPa)	$\hat{\omega}_0$ (K^{-1})	d
75.0	0.0	−4.0	1.0	120.0	0.0	10.0
$\sigma_1(T_0)$ (MPa)	ω_1 (K^{-1})	b'	n'	$\hat{\sigma}_1(T_0)$ (MPa)	$\hat{\omega}_1$ (K^{-1})	d'
300.0	0.0008	5.0	1.5	200.0	0.0	7.0
$\sigma_v(T_0)$ (MPa)	ω_v (K^{-1})	$\dot{\epsilon}_0$ (s^{-1})	m			
50.0	0.0006	1.0	5.0			

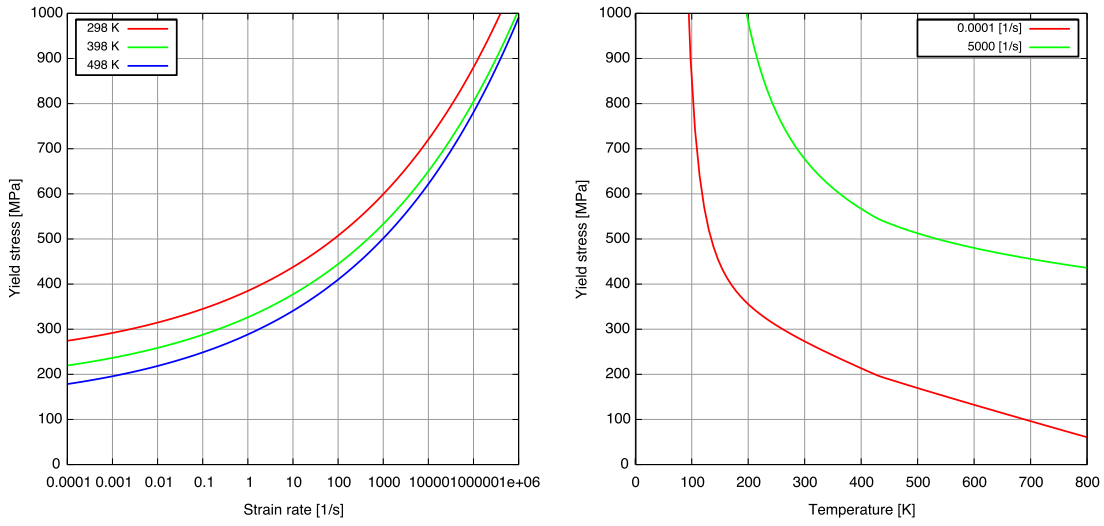

Fig. 5. Semi-logarithmic plot showing the evolution (as modeled) of initial yield stress with strain-rate and temperature, for pure polycrystalline Ta (no annealing).

Table 3
Material properties for pure polycrystalline tantalum ($T_0 = 298$ K).

G_0 (GPa)	G_1 (GPa/K)	K_0 (GPa)	K_1 (GPa/K)	α (K^{-1})	ρ_0 (kg/m^3)	C_0 (J/(kg K))
68.9	0.0	206.7	0.0	6.6×10^{-6}	16650.0	140.0
$\sigma_0(T_0)$ (MPa)	ω_0 (K^{-1})	b	n	$\hat{\sigma}_0(T_0)$ (MPa)	$\hat{\omega}_0$ (K^{-1})	d
10.0	0.0150	0.0	–	15.0	0.0	80.0
$\sigma_1(T_0)$ (MPa)	ω_1 (K^{-1})	b'	n'	$\hat{\sigma}_1(T_0)$ (MPa)	$\hat{\omega}_1$ (K^{-1})	d'
210.0	0.0018	1.25	1.0	0.0	–	–
$\sigma_v(T_0)$ (MPa)	$\dot{\epsilon}_0(T_0)$ (s^{-1})	T_c (K)	m			
125.0	0.1	4200	8.3			

Since a number of discrepancies can be observed between the various available sets of experimental results (which can be attributed to differences in material processing and/or purity levels), we have based the identification of constitutive parameters on the measurements of Rittel et al. (2007) on as-received (i.e., not annealed) Ta samples. We can nonetheless check that, when extrapolated outside the temperature and strain-rate ranges used for identification, the resulting model exhibits trends which agree well with other experimental observations (e.g., Hoge and Mukherjee, 1977 or Nemat-Nasser and Isaacs, 1997). This is illustrated in Fig. 5, showing the evolution of the initial yield stress with temperature and strain-rate, which compare qualitatively well with these other experimental observations. The complete set of constitutive parameters is given in Table 3.

In their paper, Rittel et al. (2007) presented two sets of stress–strain curves: a set of quasi-static tests on cylindrical and SCS specimens, covering the range $[10^{-4}, 10^{-1}]$ s^{-1}, and a set of dynamic tests on SCS specimens, in the range $[10^3, 10^5]$ s^{-1}. The corresponding stress–strain curves obtained with the above model and parameters are shown in Fig. 6. These numerical curves match experimental results well within the limits of experimental precision. The fitting on dynamic curves may seem of lesser quality, but it should be noted that the experimental points shown here were extracted from highly oscillatory experimental curves (due to wave reflections in the specimen).

Slow quasi-static tests correspond to long durations, and conduction effects have time to develop. It is thus reasonable to consider that these tests correspond to isothermal conditions. On the contrary, dynamic tests correspond to much shorter durations, and conduction effects play no significant role. In that case, it is reasonable to consider adiabatic conditions. Note that for intermediate strain-rates, such as in the tests at 0.11 s^{-1} (and maybe also at 0.015 s^{-1}), the actual conditions are intermediate between isothermal and adiabatic. We have nonetheless performed parameter identification under the hypothesis of isothermal conditions for all quasi-static tests. As can be seen in Fig. 7, the difference between the two extreme cases remains relatively small in terms of stress levels.

In dynamic tests, conditions are mostly adiabatic, leading to a significant temperature increase. This temperature increase was measured by Rittel et al. (2007), and these measurements are compared to the prediction of our numerical simulation in Fig. 8, for two distinct strain-rates. Note that the surprisingly low temperature increase measured at small strains was attributed (in Rittel et al. (2007)) to calibration issues of the IR sensor. Indeed, it seems otherwise difficult to explain that no significant heating is measured up to plastic strains of 5%. The agreement with numerical simulation is much better at higher strains, and we can thus consider that our model is successful in reproducing experimental observations.

4. Discussion

As already emphasized, the variational theory does not involve the *a priori* definition or modeling of a Taylor–Quinney coefficient

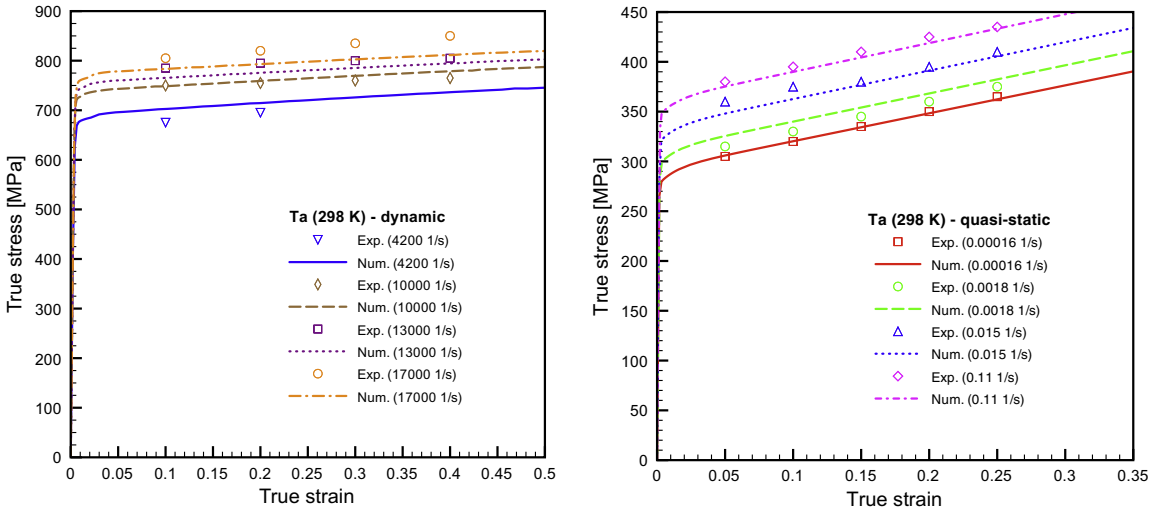

Fig. 6. Stress–strain curves for pure polycrystalline Ta (no annealing), in the quasi-static range (isothermal conditions) and dynamic range (adiabatic conditions). Experimental results taken from Rittel et al. (2007).

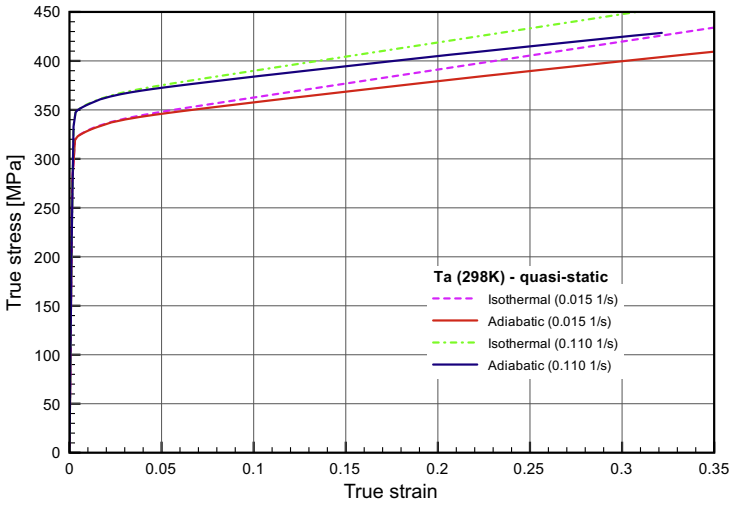

Fig. 7. Stress–strain curves for pure polycrystalline Ta (no annealing), in the upper quasi-static range: comparison between isothermal conditions and adiabatic conditions.

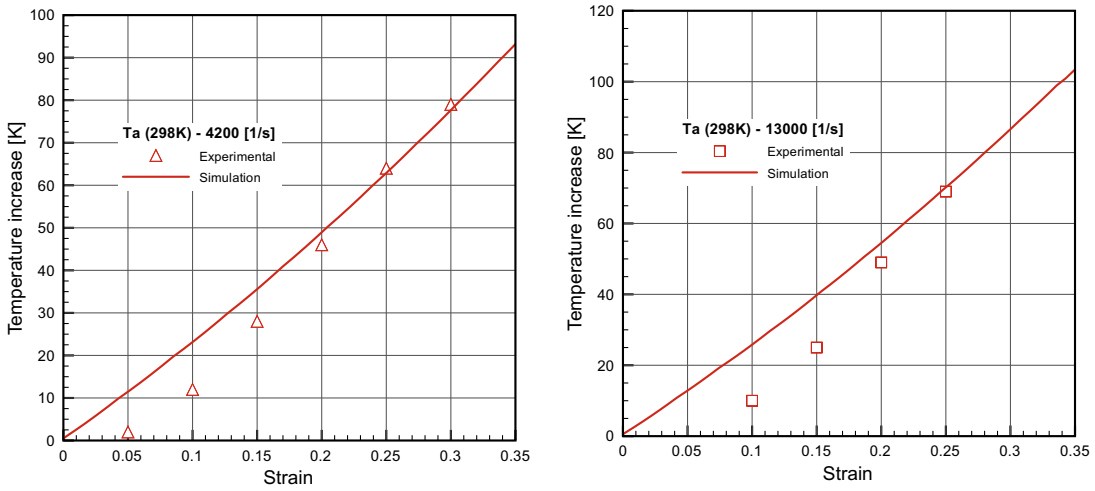

Fig. 8. Adiabatic temperature increase curves for pure polycrystalline Ta (no annealing), in the dynamic range (4200 s^{-1} and 13,000 s^{-1}). Experimental results taken from Rittel et al. (2007).

describing the partition of plastic work into dissipated heat and stored energy. Instead, the specification of the free energy potential W and the dissipation pseudo-potential ψ^* suffices to define all aspects of the material behavior, including the hardening behavior, the rate-dependence and both thermoelastic and thermoplastic coupling. It is nonetheless possible, and often illuminating, to compute *a posteriori* the evolution of the Taylor–Quinney factor *predicted* by the theory. Thus, comparison of relations (32) and (33) gives

$$\beta = \frac{1}{\boldsymbol{S}\cdot\boldsymbol{M}}\left[(\boldsymbol{S}-\boldsymbol{S}^c)\cdot\boldsymbol{M} - \frac{\partial W^{\mathrm{p}}}{\partial \bar{\epsilon}^{\mathrm{p}}}\right] \tag{48}$$

The resulting expression is in general function of both strain level and strain-rate. This is illustrated by the evolutions computed for the aluminum alloy (Fig. 9) and the titanium alloy (Fig. 10). In the case of aluminum, the initial value of β is slightly above 30%. Then, as the strain level increase, a small decrease of fraction β is first observed, rapidly followed by an increase leading above 50% for engineering strains of 40%. This shows not only that the fraction of plastic work transformed into heat is far from being constant, but also that it is not always in the range [0.8, 1.0]. In the case of titanium (Fig. 10), on the other hand, fraction β evolves between 80% and 95%, well within the traditional [0.8, 1.0] range. The mechanical behavior being rate-dependent, we now also observe a dependency of β on the strain-rate. The fraction β computed in the case of dynamic loading is indeed initially superior to the β computed in the quasi-static case, although they tend to the same value of 95% at high strains. Note again that the experimental strain range was limited to 20% in the high strain-rate case, and that this latter observation must thus be taken with caution. These numerical results are in good agreement with those computed in Hodowany et al. (2000) from experimental measurements given.

In the case of pure polycrystalline tantalum, Rittel et al. (2007), as well as others (Nemat-Nasser and Isaacs, 1997), interpreted their experimental results as supporting the assumption of a Taylor–Quinney factor equal to 1.0 (100% of plastic work transformed into heat). The evolution of the heat to plastic work fraction computed from the variational theory is shown in Fig. 11. These predictions confirm the that, for high strain-rates, the assumption that $\beta = 1$ is indeed reasonable. By contrast, Fig. 11 additionally suggests that that model does not remain valid at intermediate strain-rates. Indeed, at a strain-rate of 0.11 s^{-1}, the computed factor β is closer to 90% than 100%. As already noted, at intermediate strain-rates

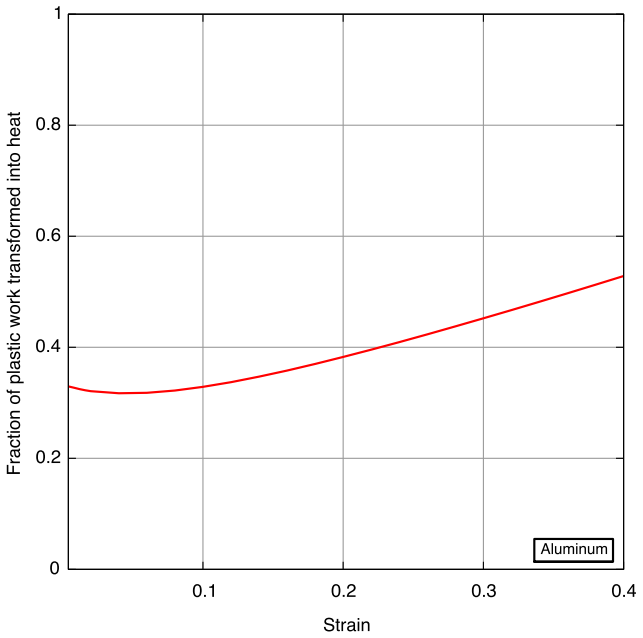

Fig. 9. Evolution with strain of fraction β of plastic work converted into heat, for rate-independent 2023-T3 aluminum alloy.

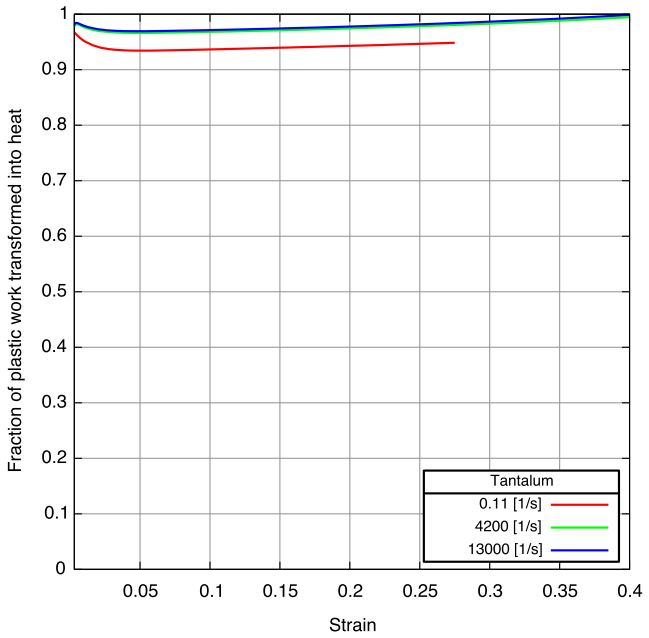

Fig. 11. Evolution with strain of fraction β of plastic work converted into heat, for pure polycrystalline tantalum (no annealing).

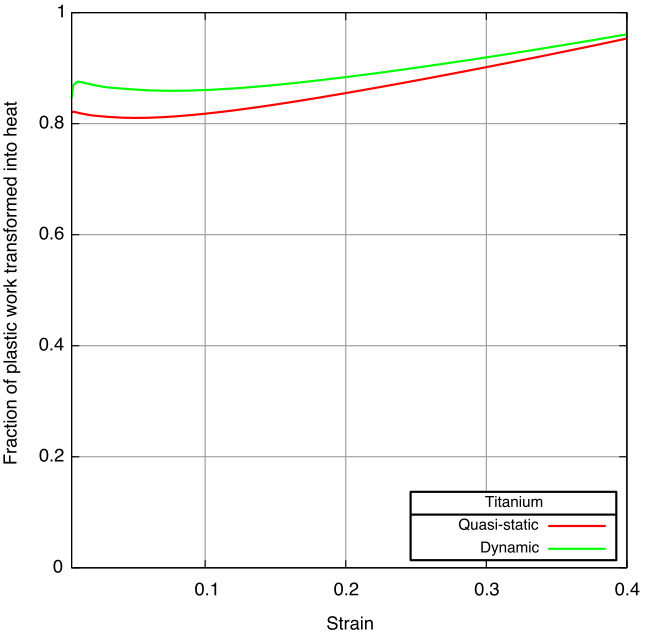

Fig. 10. Evolution with strain of fraction β of plastic work converted into heat, at two different strain rates (quasi-static at $10^{-3}\,s^{-1}$ and dynamic at $3000\,s^{-1}$) for rate-dependent α-titanium alloy.

thermal conditions are most likely to be intermediate between isothermal and adiabatic and the simple model $\beta = 1$ is likely to be too crude in that range.

In order to model β and its evolution, Rosakis et al. (2000) proposed to compute from a single experimental measurement (i.e., one stress–strain curve and one temperature–strain curve, under adiabatic conditions) a unique stored energy function which can then be used to predict thermoplastic behavior under other loading conditions. Evidently, this stored energy function is closely related to the plastic free energy $W^p(\bar{\epsilon}^p, T)$ used in the present theory, see relation (35). However, an essential difference is that the model proposed by Rosakis et al. (2000) is based on a stored energy $\overline{E}(\bar{\epsilon}^p)$ which is function of the cumulative plastic strain alone, whereas the plastic free energy is in general a function of both plastic strain and temperature. The relation between these two functions is given by

$$\overline{E}(\bar{\epsilon}^p) \equiv W^p(\bar{\epsilon}^p, T[\bar{\epsilon}^p]) \tag{49}$$

where $T[\bar{\epsilon}^p]$ is the temperature evolution in the particular loading case considered. Therefore, the stored energy function $\overline{E}(\bar{\epsilon}^p)$ is not uniquely defined in general (i.e., it is not a state function) and it cannot be used to compute the evolution of β under all other loading cases.

Despite this limitation, in cases where there is no explicit dependence of the plastic free energy on temperature the two functions coincide ($\overline{E}(\bar{\epsilon}^p) \equiv W^p(\bar{\epsilon}^p)$), and the stored energy function of Rosakis et al. (2000) indeed becomes a unique state function. In this particular case, the procedure proposed by Rosakis et al. for constructing $\overline{E}(\bar{\epsilon}^p)$ from a single adiabatic experiment is indeed very useful for purposes of deriving an expression of the plastic stored energy W^p. For the first two materials considered in this paper (Al and Ti) no significant explicit dependence of W^p on temperature is identified ($\omega_0 = \hat{\omega}_0 = 0.0$ in Tables 1 and 2), and our examples thus happen to fall in this particular case. The plastic stored energy functions corresponding to the sets of identified parameters are shown for the aluminum alloy and the titanium alloy (Fig. 12). The functions obtained here share at least a qualitative resemblance with those obtained in Rosakis et al. (2000). However, it should be carefully noted that the constitutive parameters used in the present work are identified from experimental data reported in Hodowany et al. (2000), which appear to be at variance with those reported in Rosakis et al. (2000).

By way of contrast, in the case of tantalum the plastic free energy function is explicitly dependent on temperature ($\omega_0 \neq 0$), and the stored energy function $E(\bar{\epsilon}^p)$ is not uniquely defined. This is illustrated in Fig. 13, which compares the evolution of the plastic free energy under isothermal and adiabatic conditions at various strain rates. The effect of thermal softening is evident in the figure. Thus, the stored energy function cannot be uniquely determined and the model of Rosakis et al. (2000) fails to apply.

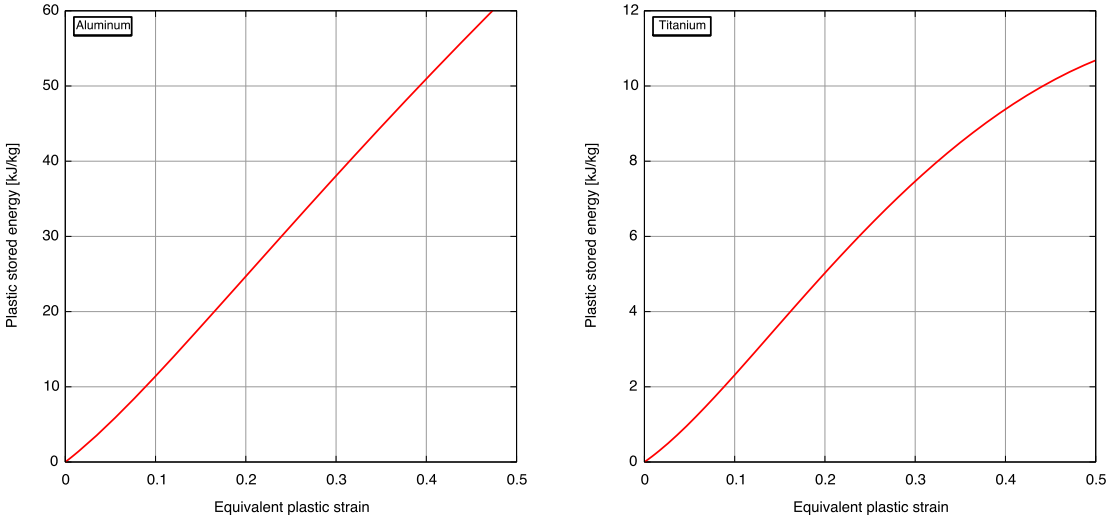

Fig. 12. Plastic stored energy function for rate-independent 2023-T3 aluminum alloy and rate-dependent α-titanium alloy.

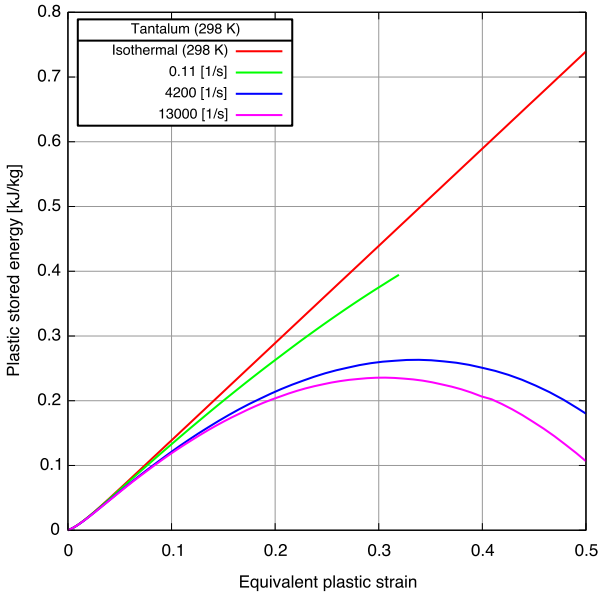

Fig. 13. Evolution of plastic stored energy function for pure polycrystalline tantalum at various strain rates, under adiabatic conditions, compared with the reference isothermal state function.

Acknowledgments

The authors gratefully acknowledge the support of the Department of Energy through Caltech's ASCI/ASAP Center for Simulating the Dynamic Response of Materials. L.S. is a Research Associate at the *Fonds de la Recherche Scientifique – FNRS*.

References

Adam, L., Ponthot, J.P., 2005. Thermomechanical modeling of metals at finite strains: first and mixed order finite elements. International Journal of Solids and Structures 42 (21–22), 5615–5655.

Aravas, N., Kim, K-S., Leckie, F.A., 1990. On the calculations of the stored energy of cold work. Journal of Engineering Materials and Technology 112 (4), 465–470.

Benzerga, A.A., Bréchet, Y., Needleman, A., Van der Giessen, E., 2005. The stored energy of cold work: predictions from discrete dislocation plasticity. Acta Materialia 53 (18), 4765–4779.

Bever, M.B., Holt, D.L., Titchener, A.L., 1973. The stored energy of cold work. Progress in Materials Science 17, 5–177.

Camacho, G.T., Ortiz, M., 1997. Adaptive Lagrangian modelling of ballistic penetration of metallic targets. Computer Methods in Applied Mechanics and Engineering 142 (3–4), 269–301.

Chaboche, J.L., 1993. Cyclic viscoplastic constitutive equations. Part II: stored energy – comparison between models and experiments. Journal of Applied Mechanics 60 (4), 822–828.

Charalambakis, N., 2001. Shear stability and strain, strain-rate and temperature-dependent "cold" work. International Journal of Engineering Science 39 (17), 1899–1911.

Chen, S.R., Gray, G.T., 1996. Constitutive behavior of tantalum and tantalum–tungsten alloys. Metallurgical and Materials Transactions A 27 (10), 2994–3006.

Chrysochoos, A., Belmahjoub, F., 1992. Thermographic analysis of thermo-mechanical couplings. Archives of Mechanics 44 (1), 55–68.

Chrysochoos, A., Maisonneuve, O., Martin, G., Caumon, H., Chezeaux, J.C., 1989. Plastic and dissipated work and stored energy. Nuclear Engineering and Design 114 (3), 323–333.

Halphen, B., Nguyen, Q.S., 1975. Sur les matériaux standard généralisés. Journal de Mécanique 14, 39–63.

Hodowany, J., Ravichandran, G., Rosakis, A.J., Rosakis, P., 2000. Partition of plastic work into heat and stored energy in metals. Experimental Mechanics 40 (2), 113–123.

Hoge, K.J., Mukherjee, A.K., 1977. The temperature and strain-rate dependence of the flow stress of tantalum. Journal of Materials Science 12 (2), 1666–1672.

Jovic, C., Wagner, D., Herve, P., Gary, G., Lazzarotto, L., 2006. Mechanical behaviour and temperature measurement during dynamic deformation on split Hopkinson bar of 304L stainless steel and 5754 aluminium alloy. Journal de Physique IV 134, 1279–1285.

Kapoor, R., Nemat-Nasser, S., 1998. Determination of temperature rise during high strain-rate deformation. Mechanics of Materials 27 (1), 1–12.

Khan, A.S., Liang, R.S., 1999. Behaviors of three bcc metal over a wide range of strain rates and temperatures: experiments and modeling. International Journal of Plasticity 15 (10), 1089–1109.

Khan, A.S., Liang, R.S., 2000. Behaviors of three bcc metals during non-proportional multi-axial loadings: experiments and modeling. International Journal of Plasticity 16 (12), 1443–1458.

Kothari, M., Anand, L., 1998. Elasto-viscoplastic constitutive equations for polycrystalline metals: application to tantalum. Journal of the Mechanics and Physics of Solids 46 (1), 51–83.

Kulkarni, Y., Knap, J., Ortiz, M., 2008. A variational approach to coarse graining of equilibrium and non-equilibrium atomistic description at finite temperature. Journal of the Mechanics and Physics of Solids 56 (4), 1417–1449.

Lee, E.H., 1969. Elastic–plastic deformations at finite strains. Journal of Applied Mechanics 36, 1–6.

Lee, B.J., Vecchio, K.S., Ahzi, S., Schoenfeld, S., 1997. Modeling the mechanical behavior of tantalum. Metallurgical and Materials Transactions A 28 (1), 113–122.

Longère, P., Dragon, A., 2008a. Plastic work induced heating evaluation under dynamic conditions: critical assessment. Mechanics Research Communications 35 (3), 135–141.

Longère, P., Dragon, A., 2008b. Evaluation of the inelastic heat fraction in the context of microstructure-supported dynamic plasticity modelling. International Journal of Impact Engineering 35 (9), 992–999.

Marusich, T.D., Ortiz, M., 1995. Modelling and simulation of high-speed machining. International Journal for Numerical Methods in Engineering 38 (21), 3675–3694.

Mason, J.J., Rosakis, A.J., Ravichandran, G., 1994. On the strain and strain-rate dependence of plastic work converted to heat: an experimental study using

high-speed infrared detectors and the Kolsky bar. Mechanics of Materials 17 (2–3), 135–145.
Nemat-Nasser, S., Isaacs, J.B., 1997. Direct measurement of isothermal flow stress of metals at elevated temperatures and high strain rates with application to Ta and Ta–W alloys. Acta Materialia 45 (3), 907–919.
Nemat-Nasser, S., Kapoor, R., 2001. Deformation behavior of tantalum and a tantalum tungsten alloy. International Journal of Plasticity 17 (10), 1351–1366.
Nemat-Nasser, S., Ni, L., Okinaka, T., 1998. A constitutive model for fcc crystals with application to polycrystalline of the copper. Mechanics of Materials 30 (4), 325–341.
Ortiz, M., Stainier, L., 1999. The variational formulation of viscoplastic constitutive updates. Computer Methods in Applied Mechanics and Engineering 171 (3–4), 419–444.
Rittel, D., Bhattacharyya, A., Poon, B., Zhao, J., Ravichandran, G., 2007. Thermo-mechanical characterization of pure polycrystalline tantalum. Materials Science and Engineering A 447 (1–2), 65–70.
Rosakis, P., Rosakis, A.J., Ravichandran, G., Hodowany, J., 2000. A thermodynamic internal variable model for the partition of plastic work into heat and stored energy in metals. Journal of the Mechanics and Physics of Solids 48 (3), 581–607.
Rusinek, A., Klepaczko, J.R., 2009. Experiments on heat generated during plastic deformation and stored energy for trip steels. Materials & Design 30 (1), 35–48.
Rusinek, A., Zaera, R., Klepaczko, J.R., 2007. Constitutive relations in 3-D for a wide range of strain rates and temperatures – application to mild steels. International Journal of Solids and Structures 44 (17), 5611–5634.
Simo, J.C., Miehe, C., 1992. Associative coupled thermoplasticity at finite strains: formulation, numerical analysis and implementation. Computer Methods in Applied Mechanics and Engineering 98, 41–104.
Stainier, L., 2007. A variational approach to thermomechanical coupling in plasticity. In: Oñate E., Papadrakakis, M., Schrefler, B. (Eds.), COUPLED PROBLEMS 2007, International Conference on Computational Methods for Coupled Problems in Science and Engineering, Ibiza, Spain, pp. 129–132.
Stainier, L., 2009. A variational finite element approach for thermo-mechanical coupling in computational structural mechanics. In: Schrefler, B., Oñate E., Papadrakaki, M. (Eds.), COUPLED PROBLEMS 2009, International Conference on Computational Methods for Coupled Problems in Science and Engineering, Ischia, Italy.
Stainier, L., Cuitiño, A.M., Ortiz, M., 2002. A micromechanical model of hardening, rate sensitivity and thermal softening in bcc single crystals. Journal of the Mechanics and Physics of Solids 50 (7), 1511–1545.
Taylor, G.I., Quinney, H., 1937. The latent heat remaining in a metal after cold working. Proceedings of the Royal Society of London, Series A 163, 157–181.
Titchener, A.L., Bever, M.B., 1958. The stored energy of cold work. Progress in Metal Physics 7, 247–338.
Voyiadjis, G.Z., Abed, F.H., 2005. Microstructural based models for bcc and fcc metals with temperature and strain rate dependency. Mechanics of Materials 37 (2–3), 355–378.
Voyiadjis, G.Z., Abed, F.H., 2006. A coupled temperature and strain rate dependent yield function for dynamic deformations of bcc metals. International Journal of Plasticity 22 (8), 1398–1431.
Weiner, J.H., 2002. Statistical Mechanics of Elasticity, second ed. Dover, New York.
Yang, Q., Stainier, L., Ortiz, M., 2006. A variational formulation of the coupled thermo-mechanical boundary-value problem for general dissipative solids. Journal of the Mechanics and Physics of Solids 54 (2), 401–424.
Zehnder, A.T., 1991. A model for the heating due to plastic work. Mechanics Research Communications 18 (1), 23–28.
Zehnder, A., Babinsky, E., Palmer, T., 1998. Hybrid method for determining the fraction of plastic work converted to heat. Experimental Mechanics 38 (4), 295–302.
Zerilli, F.J., Armstrong, R.W., 1990. Description of tantalum deformation-behavior by dislocation mechanics based constitutive relations. Journal of Applied Physics 68 (4), 1580–1591.